Influence of optical activity on rogue waves propagating in chiral optical fibers

D. D. Estelle Temgoua[1,2,3,*] and T. C. Kofane[1,2,†]

[1]*Laboratory of Mechanics, Materials and Structures, Post Graduate School in Sciences, Technology and Geosciences, Doctoral Research Unit in Physics and Applications, University of Yaounde I, P.O. Box 812, Yaounde, Cameroon*

[2]*Centre d'Excellence Africain en Technologies de l'Information et de la Communication, University of Yaounde I, P.O. Box 812, Yaounde, Cameroon*

[3]*Organization for Women in Science for the Developing World, ICTP Campus, Strada Costiera 11, 34151 Trieste, Italy*

(Received 11 January 2016; revised manuscript received 14 April 2016; published 22 June 2016)

We derive the nonlinear Schrödinger (NLS) equation in chiral optical fiber with right- and left-hand nonlinear polarization. We use the similarity transformation to reduce the generalized chiral NLS equation to the higher-order integrable Hirota equation. We present the first- and second-order rational solutions of the chiral NLS equation with variable and constant coefficients, based on the modified Darboux transformation method. For some specific set of parameters, the features of chiral optical rogue waves are analyzed from analytical results, showing the influence of optical activity on waves. We also generate the exact solutions of the two-component coupled nonlinear Schrödinger equations, which describe optical activity effects on the propagation of rogue waves, and their properties in linear and nonlinear coupling cases are investigated. The condition of modulation instability of the background reveals the existence of vector rogue waves and the number of stable and unstable branches. Controllability of chiral optical rogue waves is examined by numerical simulations and may bring potential applications in optical fibers and in many other physical systems.

DOI: 10.1103/PhysRevE.93.062223

I. INTRODUCTION

Recently, propagation phenomena of solitons [1–5] and vector solitons [6–8] in nonlinear media with natural or induced linear optical activity [9–13] have attracted more attention and have lead to important advances from the fundamental and technological point of view. More recently in optics, the study of propagation [14,15] in birefringent optical fibers allows to introduce the concept of shape-changing solitons that share energy among themselves during propagation. So, when two optical waves copropagate inside a birefringent single-mode fiber, their states of polarization change during propagation as a result of optically induced nonlinear birefringence. This polarization instability manifests itself as large changes in the output state of polarization, when the input power or the polarization state is changed slightly [16]. Those optical activities are the consequence of intrinsic linear birefringence [17] or circular birefringence [18] known as natural chirality or artificial chirality. The natural chirality is caused by the spatial dispersion of optical response either in chiral molecules or in chiral arrangements of molecules and the artificial chirality is induced by structural chirality, i.e., by artificially chiral structural features in subwavelength scale.

This notion of chirality refers to the lack of bilateral symmetry of an object and can be considered as a purely geometric property of a medium. So, chirality is a geometrical concept that describes the inability of an object and its mirror image to be superimposed solely through translations and rotations. This asymmetry of chiral molecules gives rise to optical rotation, which is an example of circular birefringence with the material possessing a different refractive index for right-hand circularly polarized and left-hand circularly polarized light. This fact is expected to play an important role in the potential application of the chiral media in the microwave and optical regimes.

In fact, several nonlinear phenomena in chiral media [9–13,18,19] have been studied over the last decade for many applications and the principle problem in working with a chiral medium is on the control of chirality level. After some investigations, it has been suggested that the use of chiral material in optical fibers may be studied with polymer optical fibers [20,21]. But after some experimental studies, scientists show that, because of organic nature of most chiral materials, some of them are not indicated at the processing temperature of silica and soft glasses; they will simply be damaged. In order to solve this problem, some investigations on the controllability of spontaneous waves in optical fiber have been done [22]. Among various solutions of spontaneous waves, the Peregrine soliton [23], Akhmediev breather [24], and Kuznetsov-Ma soliton [25] are considered as theoretical prototypes to describe the interesting phenomenon of rogue waves.

As pointed out by many scientists, rogue waves are freak waves, giant waves, monster waves, and killer waves, first observed and measured scientifically at the Draupner oil platform in the North Sea [26]. They are nonlinear single oceanic waves of extremely large amplitude, much higher than the average waves and are localized both in space and time [27–29]. They appear from nowhere and disappear without a trace and their reappearance without major shape changes gives rise to a novel appellation of rogue waves, namely rogons. Because of their more complicated way to be studied in oceans, researchers extended this strange phenomenon in optical fibers [23,30–38] for better understanding and the cause of their enormous growth became a subject of scientific research. The investigation on rogue waves dynamics argue that they arise due to modulational instability [39,40] and their occurrence has been later observed in physical systems as optical wave guides [41], capillary waves [42], Bose-Einstein

*Corresponding author: estelletemgoua@yahoo.fr
†tckofane@yahoo.com

condensates [43–46], laser-plasma interactions [47], and in econophysics [48].

As it is necessary to transmit pulses of the order of subpicosecond and femtosecond frequencies, the most adequate models to describe rogue wave phenomenon are higher-order nonlinear Schrödinger (NLS) equations, which take into account group-velocity dispersion (GVD), third-order dispersion (TOD), and nonlinear effects such as self-phase modulation (SPM), cross-phase modulation (XPM), self-steepening (SS), self-frequency shift (SFS), and four-wave mixing (FWM). Thus, many works have been carried out based on higher-order NLS equations with constant coefficients [15,49] and with varying coefficients [50]. Furthermore, rogue wave solutions have been analytically found from coupled nonlinear Schrödinger (CNLS) equations describing two-dimensional waves [43]. Apart from exact solitary waves obtained from CNLS equations in chiral optical fibers, no work has been done in chiral optical fiber for the generation of optical rogue waves. Motivate by the idea to generate the chiral optical rogue waves and to control their evolution without any chiral fiber destruction, we focus our attention on the chiral parameter to underline the properties of chiral optical fiber and indirectly to show the influence of optical activity on rogue waves.

The present paper is organized as follows. In Sec. II we show how to derive two-dimensional NLS equation in chiral optical fibers starting from Born-Fedorov equations. In Sec. III we use the symmetry reduction and the modified Darboux transformation to generate the analytical chiral optical rogue wave solutions in the presence and in the absence of management. In Sec. IV we present the influence of optical activity on the propagation of optical rogue waves, for their possible control in chiral media. In Sec. V we present the exact solutions of the chiral CNLS equations with coupled space-dependence coupling field. In Sec. VI physical properties of vector rogue waves with mixed polarization in chiral optical fiber are given. In Sec. VII we summarize the outcomes.

II. DERIVATION OF THE NONLINEAR SCHRÖDINGER EQUATION IN CHIRAL OPTICAL FIBERS

The phenomenological theory based on the Beltrami-Maxwell formalism extended to nonlinear chiral medium [10] has given rise to new effects of great significance in chiral applications. First observed in optical activity, chirality corresponds to the rotation of the polarization plane in a linear isotropic material. In an anisotropic cubic media, we add to the polarization P and/or to the magnetization M, an additional term T_c proportional to $\vec{\nabla}\times\vec{H}$, which measure per units length, the chirality. The spatial chirality effect in a medium is characterized through the Born-Fedorov formalism, based on the predicted Maxwell's equations. In chiral optical fibers, the Born-Fedorov equations are the most adequate for the study of optical activity. As they satisfy to the edge conditions [51], this allows us to characterize the nonlinear chiral medium by the given equations [9,10,12]

$$\begin{aligned}\vec{D} &= \varepsilon_n\vec{E} + \varepsilon_0 T_c\vec{\nabla}\times\vec{E},\\ \vec{B} &= \mu_0(\vec{H} + T_c\vec{\nabla}\times\vec{H}),\end{aligned} \tag{1}$$

where the flux densities $\vec{D}$ and $\vec{B}$ arise in response to the electric and magnetic field $\vec{E}$ and $\vec{H}$ propagating in the chiral medium with $\varepsilon_n = \varepsilon_0 + \varepsilon_2|\vec{E}|$. Here ε_0 and ε_2 are linear and nonlinear permittivity, respectively. μ_0 is the permeability and T_c the chiral parameter of the optical fiber. In our medium, the predicted Maxwell equations are

$$\begin{aligned}&\vec{\nabla}\cdot\vec{D} = \rho_V, \quad \vec{\nabla}\cdot\vec{B} = 0,\\ &\vec{\nabla}\times\vec{E} = -\frac{\partial\vec{B}}{\partial t}, \quad \vec{\nabla}\times\vec{H} = \vec{J} + \frac{\partial\vec{D}}{\partial t},\end{aligned} \tag{2}$$

where the current density $\vec{J} = \sigma\vec{E}$ and the charge density ρ represents the sources for the electromagnetic field. The quantity σ is the electrical conductivity and V the volume. Substituting Eq. (1) into Eq. (2), we obtain the following wave equation

$$\begin{aligned}&\nabla^2\vec{E} + \mu_0\varepsilon_0 {T_c}^2\frac{\partial^2\nabla^2\vec{E}}{\partial t^2}\\ &= \mu_0\varepsilon_0\frac{\partial^2\vec{E}}{\partial t^2} + \mu_0\sigma\frac{\partial\vec{E}}{\partial t} + \mu_0\varepsilon_2|\vec{E}|\frac{\partial^2\vec{E}}{\partial t^2}\\ &\quad + 2\mu_0\varepsilon_0 T_c\vec{\nabla}\times\frac{\partial^2\vec{E}}{\partial t^2} + \mu_0\varepsilon_2 T_c|\vec{E}|^2\vec{\nabla}\times\frac{\partial^2\vec{E}}{\partial t^2}\\ &\quad + \mu_0\sigma T_c\vec{\nabla}\times\frac{\partial\vec{E}}{\partial t}.\end{aligned} \tag{3}$$

The optical field $\vec{E}$ is represented by a right- (R) or left-hand (L) polarization in the z direction as

$$\begin{aligned}\vec{E}(\vec{r},t) &= (\hat{x}\mp j\hat{y})\vec{A}(\vec{r},t)\exp[-j(K_\pm z - \omega_0 t)]\\ &= \vec{\psi}_{R,L}\exp[-j(K_\pm z - \omega_0 t)],\end{aligned} \tag{4}$$

where $\vec{\psi}_{R,L}$ is the complex envelope of the optical field in the nonlinear chiral medium, K the wave number, and ω_0 the frequency.

After evaluation of different derivations of $\vec{E}$ in x, y, and z directions in Eq. (3), we neglect the second-order terms and suppose that the wave is propagating in the z direction. This imply that

$$K_x = K_y = 0, \quad E_z = 0. \tag{5}$$

Considering the slowly varying envelope of the amplitude, we can do the paraxial approximation bellow

$$\begin{aligned}\left|\frac{\partial^2 E_x}{\partial z^2}\right| &\ll \left|2jK_z\frac{\partial E_x}{\partial z}\right|,\\ \left|\frac{\partial^2 E_y}{\partial z^2}\right| &\ll \left|2jK_z\frac{\partial E_y}{\partial z}\right|.\end{aligned} \tag{6}$$

The final result of Eq. (3), after approximations, stands for (see the Appendix)

$$\begin{aligned}&j\frac{\partial\phi}{\partial z'} + \frac{1}{2}K''\frac{\partial^2\phi}{\partial t'^2} - j\frac{1}{6}K'''\frac{\partial^3\phi}{\partial t'^3} + j\frac{\omega\alpha}{2K_0}(1\mp KT_c)\phi\\ &- \frac{\beta\omega^2}{2K_0}(1\mp KT_c)|\phi|^2\phi \mp K^2T_c\phi + j\frac{\omega\beta}{K_0}|\phi|^2\frac{\partial\phi}{\partial t'} = 0,\end{aligned} \tag{7}$$

where $K' = \frac{\partial K}{\partial \omega} = \frac{1}{v_g}$ is the inverse of group velocity $K'' = \frac{\partial K'}{\partial \omega}$ is the group-velocity dispersion coefficient, which takes the plus and minus signs ($\pm$), representing the anomalous and normal dispersion regimes, respectively. The parameter $K''' = \frac{\partial K''}{\partial \omega}$ is the TOD term. In the fourth term, the attenuation coefficient α is weighted towards the chiral parameter T_c. The factor to $|\phi|^2\phi$ is the SPM and the term $K^2 T_c \phi$ occurs as an additional correction to the chirality of the fiber. The last term has the physical sense of SS and is necessary to perform the description of spontaneous waves.

The new variables, namely

$$
\begin{aligned}
q &= \frac{{\omega_0}^{2/3}\beta^{1/3}}{(2K_0)^{1/3}}\phi, \quad \xi = \frac{{\omega_0}^{2/3}\beta^{1/3}}{(2K_0)^{1/3}}z' \\
\tau &= \frac{{\omega_0}^{1/3}\beta^{1/16}}{\sqrt{K''}(2K_0)^{1/6}}t', \quad \Gamma = \frac{{\omega_0}^{1/3}\alpha}{(2K_0)^{1/3}\beta^{1/3}} \\
\gamma &= \frac{\beta^{1/6}K'''}{6K''}\frac{{\omega_0}^{1/3}}{\sqrt{(2K_0)^{1/3}K''}}, \quad C = 1 \mp T_c K \\
D &= \frac{K^2 T_c (2K_0)^{1/3}}{\beta^{1/3}{\omega_0}^{2/3}}, \quad \alpha_3 = \frac{(2K_0)^{5/6}\beta^{1/6}}{\sqrt{K''}{\omega_0}^{2/3}K_0}
\end{aligned}
\tag{8}
$$

allow us to express Eq. (7) in the form

$$
\begin{aligned}
& j\frac{\partial q}{\partial \xi} + \frac{1}{2}\frac{\partial^2 q}{\partial \tau^2} - j\gamma\frac{\partial^3 q}{\partial \tau^3} + jC\Gamma q \mp Dq - C|q|^2 q \\
& + j\alpha_3 |q|^2 \frac{\partial q}{\partial \tau} = 0.
\end{aligned}
\tag{9}
$$

Equation (9) is the NLS equation for a chiral optical fiber. This generalized chiral NLS equation can be used to describe the propagation of right-hand (+) and left-hand (−) polarized rogue waves in a higher-order dispersive and nonlinear chiral optical fiber. If we let $\alpha_3 = 0$, we obtain another form of NLS equation for a chiral optical fiber without the SS term [10]. For $T_c = 0$, $C = 1$, $D = 0$, $\gamma = 0$, and $\Gamma = 0$, Eq. (9) stands for the standard NLS equation.

If we let $q(\xi,\tau) = \psi(\xi,\tau)$, $\varphi = \frac{1}{2}$, and $\mu = C\Gamma$, the model becomes

$$
\begin{aligned}
& j\frac{\partial \psi}{\partial \xi} + \varphi\frac{\partial^2 \psi}{\partial \tau^2} - j\gamma\frac{\partial^3 \psi}{\partial \tau^3} + j\mu\psi \mp D\psi - C|\psi|^2\psi \\
& + j\alpha_3 |\psi|^2 \frac{\partial \psi}{\partial \tau} = 0.
\end{aligned}
\tag{10}
$$

We should keep in mind that the controllability condition should be verified in Eq. (10). With the aim of taking into account the missing condition of controllability (on higher-order NLS models) Yan *et al.* [52] showed that the sum of parameters related to the SS, that is, a_2 and to the SFS, that is, a_3 should be zero: $a_2 + a_3 = 0$. In order to achieve this aim, let us write the sum of the SS (α_3) and the SFS (α_4) in the following form

$$
\begin{aligned}
& j[\alpha_3(|\psi|^2\psi)_\tau + \alpha_4\psi(|\psi|^2)_\tau] \\
& \quad = j[\alpha_3|\psi|^2\psi_\tau + (\alpha_3+\alpha_4)\psi(|\psi|^2)_\tau]
\end{aligned}
\tag{11}
$$

and let $\alpha_3 + \alpha_4 = 0$; it will remain another term of SS given by $j\alpha_3|\psi|^2\psi_\tau$. Thus, the assumption of controllability is verified by the model given in Eq. (10). Our main aim now is to find the rational solutions of Eq. (10) with variable and constant coefficients, which may be useful to control the propagation of chiral optical rogue waves.

III. SYMMETRY REDUCTION, FIRST- AND SECOND-ORDER RATIONAL SOLUTIONS OF THE CHIRAL NONLINEAR SCHRÖDINGER EQUATION WITH VARIABLE AND CONSTANT COEFFICIENTS

In the presence of management in Eq. (10), the optical pulse propagation in chiral media can be described by the chiral NLS equation with variable coefficients, in the form

$$
\begin{aligned}
& j\frac{\partial \psi}{\partial \xi} + \varphi(\xi)\frac{\partial^2 \psi}{\partial \tau^2} - j\gamma(\xi)\frac{\partial^3 \psi}{\partial \tau^3} + j\mu(\xi)\psi \\
& \mp D(\xi)\psi - C(\xi)|\psi|^2\psi + j\alpha_3(\xi)|\psi|^2\frac{\partial \psi}{\partial \tau} = 0,
\end{aligned}
\tag{12}
$$

where τ is taken as time parameter and ξ as spatial parameter. The variable coefficients $\varphi(\xi)$, $\gamma(\xi)$, $\mu(\xi)$, $D(\xi)$, $C(\xi)$, and $\alpha_3(\xi)$ are related to the GVD, TOD, the gain and loss term of the induced optical activity, linear birefringence, SPM, and SS coefficients, respectively.

Since Eq. (12) has varying coefficients, it becomes not integrable and this strongly affects the wave propagation in chiral optical fiber. In order to solve this problem of nonintegrability of the model, we can either use the symmetry reduction method using third-order propagation vector field [53] or the envelope field in gauge form [54] to obtain some integrability conditions. This method has been applied in NLS models to look for exact analytical solutions and is the most adequate method for the construction of rogue wave solutions. From this preliminary method, varying coefficients are obtained but the complex field is deduced from the modified Darboux transformation or from the Lax pair method [55]. In what follows, we use the envelope field in the form [52,56,57]

$$
\psi(\xi,\tau) = A(\xi)V[Z(\xi),T(\xi,\tau)]\exp\{i\rho(\xi,\tau)\}
\tag{13}
$$

to construct the rational solutions related to chiral optical rogue waves, where $A(\xi)$ is the amplitude, $Z(\xi)$ the effective propagation distance, $T(\xi,\tau)$ the similitude variable, and $V[Z(\xi),T(\xi,\tau)]$ the complex field. The variable $\rho(\xi,\tau)$ is the phase of the wave. This form of envelope field is also known as the similarity transformation or the reduction method.

Substituting Eq. (8) into Eq. (13) gives a couple system of partial differential equations with variable coefficients

$$
\begin{aligned}
& -\gamma A V_T T_{\tau\tau\tau} + 3\gamma A V T_\tau {\rho_\tau}^2 + A V_T T_\xi \\
& + A V_T T_\tau \rho_\tau - \gamma A V_{TTT} {T_\tau}^3 + 3\gamma A V \rho_{\tau\tau}\rho_\tau \\
& + A_\xi V + \mu V + A V_Z Z_\xi + \varphi A V \rho_{\tau\tau} \\
& + \alpha_3 A^2 |V|^2 A V_T T_\tau - 3\gamma A V_{TT} T_\tau T_{\tau\tau} = 0,
\end{aligned}
\tag{14}
$$

$$
\begin{aligned}
& -A V \rho_\xi + \varphi A V_{TT} {T_\tau}^2 + \varphi A V_T T_{\tau\tau} - \varphi A V {\rho_\tau}^2 \\
& + \gamma A V \rho_{\tau\tau\tau} + 3\gamma A V_T T_{\tau\tau}\rho_\tau + 3\gamma A V_T T_\tau \rho_{\tau\tau} \\
& - \gamma A V {\rho_\tau}^3 + 3\gamma A V_{TT} T_\tau {}^2 \rho_\tau - \alpha_3 A^2 |V|^2 A V_T \rho_\tau \\
& \mp DAV - CA^2|V|^2 AV = 0.
\end{aligned}
\tag{15}
$$

In order to simplify the script of differential equations above, we write $A(\xi)=A$, $Z(\xi)=Z$, $T(\xi,\tau)=T$, $\rho(\xi,\tau)=\rho$. According to the previous works [52,57], we use the symmetry transformation given by Eq. (13) that would reduce Eq. (12) to the integrable Hirota equation in the form [58]

$$i\frac{\partial V}{\partial Z}=-\frac{\partial^2 V}{\partial T^2}+G|V|^2V+2\sqrt{2}i\nu\left(\frac{\partial^3 V}{\partial T^3}+3|V|^2\frac{\partial V}{\partial T}\right). \tag{16}$$

In the case of rogue waves finding, we take $G=-1$. The parameter ν is a real constant. With $V[Z(\xi),T(\xi,\tau)]$ satisfying the relation (16), the similarity reduction of Eqs. (14) and (15) leads to

$$\gamma(\xi)T_\tau T_{\tau\tau}=0, \tag{17}$$

$$\varphi(\xi)T_{\tau\tau}+3\gamma(\xi)(T_{\tau\tau}\rho_\tau+T_\tau\rho_{\tau\tau})=0, \tag{18}$$

$$\mp D(\xi)+\rho_\xi+\varphi(\xi){\rho_\tau}^2+\gamma(\xi)({\rho_\tau}^3-\rho_{\tau\tau\tau})=0, \tag{19}$$

$$A_\xi+A[\varphi(\xi)\rho_{\tau\tau}+3\gamma(\xi)\rho_{\tau\tau}\rho_\tau+\mu(\xi)]=0, \tag{20}$$

$$T_\xi+T_\tau\rho_\tau-\gamma(\xi)\left(T_{\tau\tau\tau}-3T_\tau{\rho_\tau}^2\right)=0, \tag{21}$$

$$Z_\xi+{T_\tau}^2[\varphi(\xi)+3\gamma(\xi)\rho_\tau]=0, \tag{22}$$

$$\gamma(\xi){T_\tau}^3+2\sqrt{2}\nu Z_\xi=0, \tag{23}$$

$$A^2[C(\xi)+\alpha_3(\xi)\rho_\tau]+GZ_\xi=0, \tag{24}$$

$$\alpha_3(\xi)A^2T_\tau-6\sqrt{2}\nu Z_\xi=0. \tag{25}$$

Here, the subscripts ξ and τ denote spatial and temporal derivatives, respectively. The resolution of the system (17)–(25) yields for $\gamma(\xi)\neq 0$ and $T_\tau T_{\tau\tau}=0$ to the similarity variable

$$T(\xi,\tau)=T_1(\xi)\tau+T_0(\xi), \tag{26}$$

where $T_{1_\xi}(\xi)=0$. The substitution of Eq. (26) into Eq. (18) tends to $3\gamma(\xi)T_\tau\rho_{\tau\tau}=0$. As $\gamma(\xi)\neq 0$, $T_1(\xi)\neq 0$, and $\rho_{\tau\tau}=0$, the phase can be written as

$$\rho(\xi,\tau)=\rho_1(\xi)\tau+\rho_0(\xi), \tag{27}$$

where $\rho_{1_\xi}(\xi)=0$.

From Eq. (23), the effective propagation distance $Z(\xi)$ will be

$$Z(\xi)=-\frac{\sqrt{2}}{4\nu}\int_0^\xi \gamma(s){T_1(s)}^3ds. \tag{28}$$

Equation (22) stands for

$$\varphi(\xi)=-\gamma(\xi)\left(3\rho_1(\xi)-\frac{T_1(\xi)}{2\sqrt{2}\nu}\right). \tag{29}$$

Through Eq. (21), we arrive at

$$\gamma(\xi)=-\left(\frac{T_{0_\xi}(\xi)+T_1(\xi)\rho_1(\xi)}{3T_1(\xi){\rho_1}^2(\xi)}\right). \tag{30}$$

Relation (20) is transformed to

$$A(\xi)=A_0\exp\left\{-\int_0^\xi \mu(s)ds\right\}, \tag{31}$$

where, A_0 is a constant. The result coming from Eq. (21), is out to be

$$\mp D(\xi)=-\left\{\gamma(\xi){\rho_1}^2(\xi)\left(2\rho_1(\xi)-\frac{T_1(\xi)}{2\sqrt{2}\nu}\right)-\rho_{0_\xi}(\xi)\right\}, \tag{32}$$

with $D_-(\xi)=-D_+(\xi)$. Equation (25) gives the result

$$\alpha_3(\xi)=-3\gamma(\xi){T_1}^2(\xi)A^{-2}(\xi). \tag{33}$$

Through relation (24), one finds that

$$C(\xi)=\gamma(\xi){T_1}^2(\xi)\left(3\rho_1(\xi)+\frac{GT_1(\xi)}{2\sqrt{2}\nu}\right)A^{-2}(\xi). \tag{34}$$

The TOD parameter $\gamma(\xi)$ is used to control the effective propagation distance $Z(\xi)$, the GVD parameter $\varphi(\xi)$, the coefficient of linear birefringence $D(\xi)$, the SS coefficient $\alpha_3(\xi)$, and the SPM nonlinearity $C(\xi)$. The gain and loss term of the induce optical activity $\mu(\xi)$ can be used to manage the optical activity on the amplitude $A(\xi)$, on the SS coefficient $\alpha_3(\xi)$, and on the SPM nonlinearity $C(\xi)$. To determine the complex field $V[Z(\xi),T(\xi,\tau)]$, we use the modified Darboux transformation method [43,59–61]. The first- and second-order rational solutions of the Hirota equation, namely by Eq. (16), were recently found by Ankiewicz *et al.* [58]. They showed how to construct the hierarchy of rational solutions of the Hirota equation. According to the modified Darboux transformation, the first- and second-order rational solutions are constructed in the following paragraph.

Considering the correspondence $Z(\xi)=x$, $\frac{1}{\sqrt{2}}T(\xi,\tau)=t$, and $\nu=\alpha_3$ in Ref. [58], the first-order of the complex field $V[Z(\xi),T(\xi,\tau)]$ leads to

$$V_1[Z(\xi),T(\xi,\tau)]=\left[1-\frac{G_1+iH_1}{D_1}\right]\exp\{iZ(\xi)\}, \tag{35}$$

where

$$G_1=4,\quad H_1=8Z(\xi),$$
$$D_1=1+[\sqrt{2}T(\xi,\tau)+12\nu Z(\xi)]^2+4Z(\xi)^2. \tag{36}$$

Taking into account the above correspondence, solution (35) is known as the Peregrine soliton [23]. Then, collecting the partial solutions together, we construct the first-order rational solution related to the exact chiral optical rogue wave solution of Eq. (12)

$$\psi_1=A(\xi)\left[1-\frac{G_1+iH_1}{D_1}\right]\exp\{iZ(\xi)+i\rho(\xi,\tau)\}. \tag{37}$$

The intensity of the first-order chiral optical rogue wave is

$$|\psi_1|^2={A_0}^2\exp\left\{-2\int_0^\xi \mu(s)ds\right\}\times\left[\frac{([\sqrt{2}T+12\nu Z]^2+4Z^2-3)^2+64Z^2}{(1+[\sqrt{2}T+12\nu Z]^2+4Z^2)^2}\right]. \tag{38}$$

This first-order rational solution is used to describe the propagation of rogue wave in chiral optical fibers. We use it to show the influence of optical activity on the propagation of rogue waves and with a suitable choice of parameters of the original Eq. (12), we manage the controllability of chiral optical rogue wave.

Then the second-order rational solution of the complex field $V[Z(\xi),T(\xi,\tau)]$ presented by Ankiewicz *et al.* [58] stands for

$$V_2[Z(\xi),T(\xi,\tau)] = \left[1 + \frac{G_2 + iZ(\xi)H_2}{D_2}\right] \exp i\{Z(\xi)\}, \tag{39}$$

where G_2, H_2 and D_2 are given by the relations

$$\begin{aligned}
G_2 &= -48T^4 - 1152\sqrt{2}\nu ZT^3 - 144T^2[4Z^2(36\nu^2+1)+1] - 576\sqrt{2}\nu ZT[12Z^2(12\nu^2+1)+7] \\
&\quad - 192Z^4[216(6\nu^4+\nu^2)+5] - 864Z^2(44\nu^2+1) - 36, \\
H_2 &= -96T^4 - 2304\sqrt{2}\nu ZT^3 - 96T^2[4Z^2(108\nu^2+1)-3] - 1152\sqrt{2}\nu ZT[4Z^2(36\nu^2+1)] - 384Z^4(36\nu^2+1)^2 \\
&\quad - 192Z^2(180\nu^2+1) + 360, \\
D_2 &= 8T^6 + 288\sqrt{2}\nu ZT^5 - 432Z^4(624\nu^4 - 40\nu^2 - 1) + 36Z^2(556\nu^2+11) + 9 + 64Z^6(36\nu^2+1)^3 \\
&\quad + 96\sqrt{2}ZT^3[12Z^2(60\nu^2+1)-1] + 12T^4[4Z^2(180\nu^2+1)+1] + 6T^2[16Z^4[216\nu^2(30\nu^2+1)-1] \\
&\quad - 24Z^2(60\nu^2+1)+9] + 72\sqrt{2}\nu ZT[16Z^4(36\nu^2+1) + 8Z^2(1-108\nu^2) + 17].
\end{aligned} \tag{40}$$

According to the same correspondence of variables as for first-order, we obtain the second-order solution found by Akhmediev *et al.* [62]. Collecting the partial solutions together, we construct the final second-order rational solution related to the exact solution of Eq. (12)

$$\psi_2 = A(\xi)\left[1 + \frac{G_2 + iZ(\xi)H_2}{D_2}\right] \exp\{iZ(\xi) + i\rho(\xi,\tau)\}. \tag{41}$$

The intensity of the second-order chiral optical rogue wave solution is

$$\begin{aligned}
|\psi_2|^2 &= {A_0}^2 \exp\left\{-2\int_0^\xi \mu(s)ds\right\} \\
&\quad \times \left[\frac{(G_2+D_2)^2 + Z(\xi)^2{H_2}^2}{{D_2}^2}\right].
\end{aligned} \tag{42}$$

This second-order rational solution is more precise than the first one. It describes the optical activity effect on two rogue waves propagating in a chiral optical fiber as well as collisions between them. We use it in the next section to investigate the features of chirality on rogue wave collisions.

Now, we turn our attention to the case of chiral NLS equation with constant coefficients. Then, the new variables of the first- and second-order rational solutions become

$$\begin{aligned}
T(\xi,\tau) &= T_1(\xi)\tau + T_0(\xi), \\
\rho(\xi,\tau) &= \rho_1(\xi)\tau + \rho_0(\xi), \\
Z(\xi) &= -\frac{\sqrt{2}\gamma}{4\nu}\int_0^\xi T_1(s)^3 ds, \\
A(\xi) &= A_0 \exp\{-\mu\xi\},
\end{aligned} \tag{43}$$

where, $T_{1_\xi}(\xi) = 0$, $\rho_{1_\xi}(\xi) = 0$, and $\mu = b_3(1 \pm KT_c)$. By taking into account the new variables above, the first- and second-order rational solutions of the chiral NLS equation with constant coefficients are given by Eq. (37) and Eq. (41), respectively. With these exact solutions, we can appreciate the influence of optical activity on rogue wave in chiral NLS equation with constant coefficients.

After the construction of the above exact solutions, we can choose their parameters to investigate the dynamics behavior and the features of chiral optical rogue waves. So doing, we alternate the sign of values in both space and time, which is required to optimize the eventual stability of the solutions.

IV. OPTICAL ACTIVITY EFFECTS ON THE PROPAGATION OF ROGUE WAVES

To illustrate the effect of optical activity on the propagation of rogue waves related to the first- and second-order rational solutions, we choose, appropriately, free functions $T_1(\xi)$, $T_0(\xi)$, $\mu(\xi)$, and $\gamma(\xi)$ to generate abundant structures of chiral optical rogue waves. We present managed cases, in which the choice of chiral parameter leads to the control of chiral optical rogue waves. We note that parameters are chosen in order to be bounded in the intervals $-15 < \xi < 15$ and $-15 < \tau < 15$. In this work, curves are plotted with the help of MATLAB. Through Jacobian elliptic functions, the intensities of the first- and second-order rational solutions are used to show the influence of optical activity on the structure of chiral optical rogue waves. Their approximative formulas are given in reference by [63]

$$\begin{aligned}
dn(z,k) &\approx 1 - \frac{k^2\sin(z)^2}{2}, \\
cn(z,k) &\approx \cos(z) - k^2\sin(z)\left(\frac{z - \sin(z)\cos(z)}{4}\right), \\
sn(z,k) &\approx \sin(z) - k^2\cos(z)\left(\frac{z - \sin(z)\cos(z)}{4}\right).
\end{aligned} \tag{44}$$

In order to generate more stable chiral optical rogue waves, we use the Jacobian elliptic functions, which are responsible for the snaker form of waves as seen in Figs. 1, 2, and 3, where $|\psi_-|^2$ and $|\psi_+|^2$ are chiral optical rogue waves in the left- and right-hand side, respectively. We observe through these figures that when the chiral parameter T_c is weak, the waves in both hands have the same form [Figs. 1(b), 2(b), and 3(b)] and the same amplitude [Figs. 2(b) and 3(b)]. We notice that the increase of chiral parameter reveals a notable difference on the

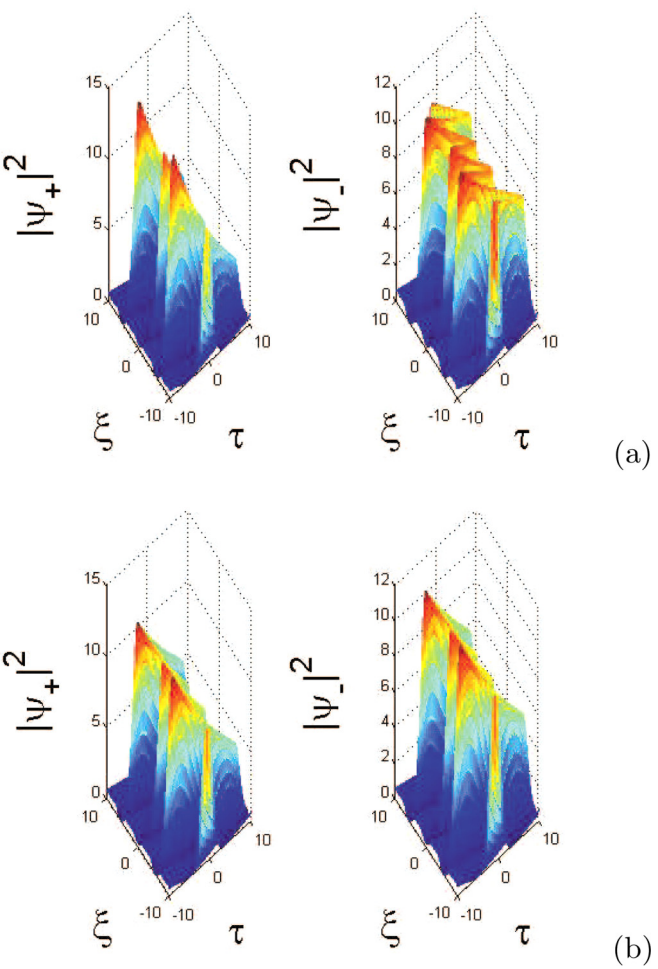

FIG. 1. First-order chiral optical rogue waves on the left- and right-hand side with variable coefficients, where the parameters are (a) $T_c = 0.5$; (b) $T_c = 0.1$; with $b_1 = 0.2$, $K = 1$, $b_3 = 0.1$, $\nu = 0.6$, $k_3 = 0.6$, $k_4 = 0.9$, $T_1(\xi) = \sqrt{2}b_1$, $T_0(\xi) = cn(\xi,k_4)$, $\gamma(\xi) = {k_3}^2 sn(\xi,k_3)cn(\xi,k_3)$ in each case and $\mu(\xi) = b_3(1 - KT_c)sn(\xi,k_4)dn(\xi,k_4)$ for the left-hand intensity $|\psi_-|^2$ and $\mu(\xi) = b_3(1 + KT_c)sn(\xi,k_4)dn(\xi,k_4)$ for the right-hand intensity $|\psi_+|^2$.

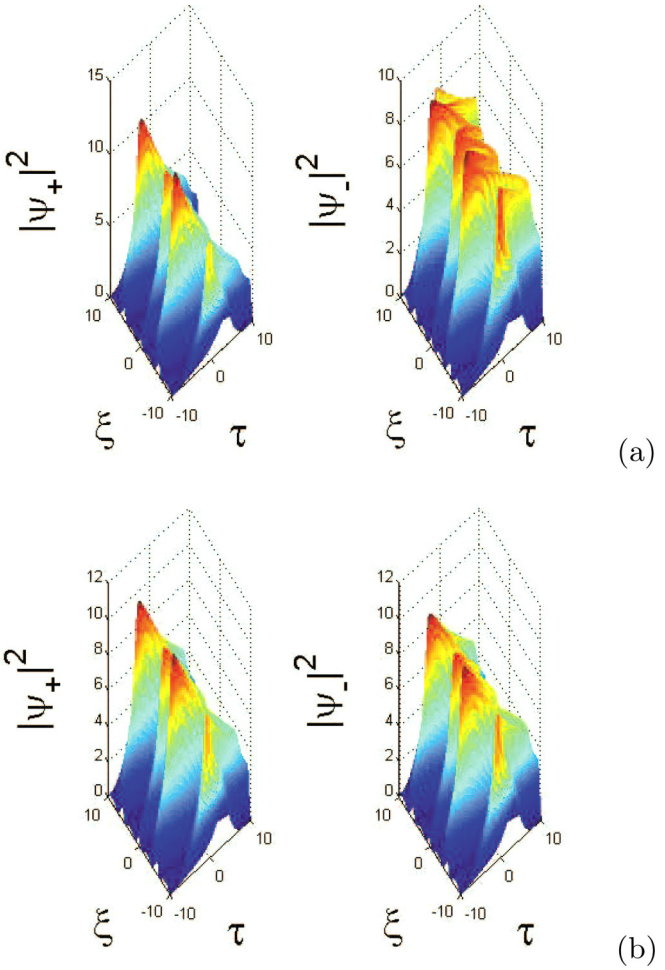

FIG. 2. Second-order chiral optical rogue waves on the left- and right-hand side with variable coefficients, where the parameters are (a) $T_c = 0.5$; (b) $T_c = 0.1$; with $b_1 = 0.2$, $K = 1$, $b_3 = 0.1$, $\nu = 0.6$, $k_3 = 0.6$, $k_4 = 0.9$, $T_1(\xi) = \sqrt{2}b_1$, $T_0(\xi) = cn(\xi,k_4)$, $\gamma(\xi) = {k_3}^2 sn(\xi,k_3)cn(\xi,k_3)$ in each case and $\mu(\xi) = b_3(1 - KT_c)sn(\xi,k_4)dn(\xi,k_4)$ for the left-hand intensity $|\psi_-|^2$ and $\mu(\xi) = b_3(1 + KT_c)sn(\xi,k_4)dn(\xi,k_4)$ for the right-hand side intensity $|\psi_+|^2$.

form of waves between the left- and right-hand intensities [see Figs. 1(a), 2(a), and 3(a)]. We denote that the second-order solutions [Figs. 2 and 3(b)] with more curvatures than the first-order solutions [Figs. 1 and 3(a)] and this, in addition to the coefficients with management, yields a more accurate study of the influence of the optical activity on rogue waves. We can conclude that the increase of the right-hand intensities and the decrease of the left-hand intensities are slightly due to the order of the solution and highly caused by the increase of the optical activity [see Figs. 2 and 3]. The exchange of energy observed here is also due to the two-wave mixing (TWM) effect. The main difference between parameters of Figs. 1–3 depends on the order of rational solutions through the parameters G_i, H_i, and D_i $(i = 1,2)$. The parameters G_1, H_1, and D_1 given in Eq. (36) have been used to construct the first-order rational solution (37) while G_2, H_2, and D_2 given in Eq. (40) have been used to construct the second-order rational solution (41) and where the parameters μ and γ depend on the variable ξ in Figs. 1 and 2. In contrast, in Fig. 3, where we have also constructed the first- and second-order rational solutions, the parameters μ and γ are constants. In order to perform this study, we use the chiral CNLS equations in what follows.

V. CHIRAL OPTICAL VECTOR ROGUE WAVES IN COUPLED NLS EQUATIONS WITH COUPLED SPACE-DEPENDENCE COUPLING FIELD

From the model obtain in Eq. (9), the coupled system of NLS equation in chiral optical fibers with coupled space-dependence coupling field is given by

$$\begin{aligned} &i\psi_{1\xi} + \varphi\psi_{1\tau\tau} - i\gamma\psi_{1\tau\tau\tau} + i\mu\psi_1 \mp D\psi_1 - (C_1|\psi_1|^2 \\ &\quad + C|\psi_2|^2)\psi_1 + i\alpha_3|\psi_1|^2\psi_{1\tau} - \beta(\xi)\psi_2 = 0, \\ &i\psi_{2\xi} + \varphi\psi_{2\tau\tau} - i\gamma\psi_{2\tau\tau\tau} + i\mu\psi_2 \mp D\psi_2 - (C|\psi_1|^2 \\ &\quad + C_2|\psi_2|^2)\psi_2 + i\alpha_3|\psi_2|^2\psi_{2\tau} - \beta(\xi)\psi_1 = 0, \end{aligned} \tag{45}$$

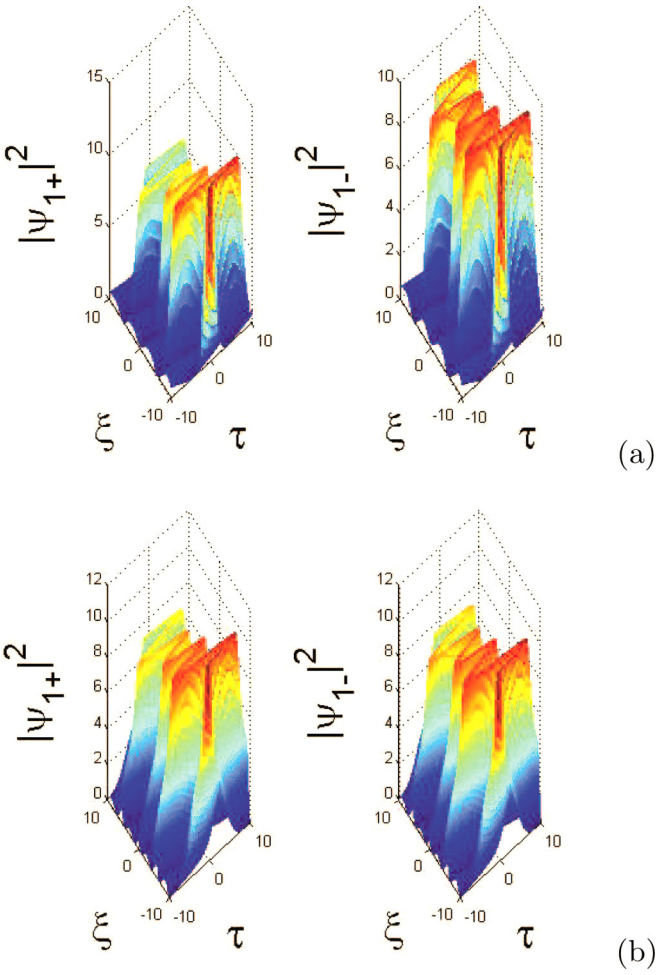

FIG. 3. (a) First- and (b) second-order chiral optical rogue waves on the right- and left-hand side with constant coefficients, where parameters are (a) $T_c = 0.5$; (b) $T_c = 0.1$; with $b_1 = 0.2$, $K = 1$, $b_3 = 0.01$, $\nu = 0.6$, $\gamma = 0.03$, $k_4 = 0.9$, $T_1(\xi) = \sqrt{2}b_1$, $T_0(\xi) = cn(\xi,k_4)$ in each case and $\mu = b_3(1 - KT_c)$ for the left-hand intensity $|\psi_-|^2$ and $\mu = b_3(1 + KT_c)$ for the right-hand intensity $|\psi_+|^2$.

where the last term $\beta(\xi)$ describes the coupling between mixed polarizations. As we consider an isotropic medium with circular polarization and linear birefringence, the presence of FWM becomes implicit through the reference changing [see Appendix (A7)] whereas the SPM terms $(C_1|\psi_1|^2\psi_1; C_2|\psi_2|^2\psi_2)$ and XPM terms $(C|\psi_1|^2\psi_2; C|\psi_2|^2\psi_1)$ can be identified in the above model. In fact, C_1 and C_2 are SPM nonlinearities (interactions) and C is the XPM nonlinearity (interactions). The FWM in our system will be responsible for the exchanging of energy between components.

Our study is based on the theory of determinant of the nonlinear coefficients in the form [43]

$$\Delta = C_1C_2 - C^2, \tag{46}$$

which determines the thermodynamic instability of the system. In order to reduce the number of figures, we choose only one value of the chiral parameter $T_c = 0.5$ and the case where the SPM interactions have the same signs of the scattering length, i.e., when $C_1C_2 > 0$ or the opposite signs.

A. Chiral optical rogue waves in the case: $\Delta = 0$

1. *First case:* $\Delta = 0$ *and* $CC_{1,2} > 0$

In this case, the XPM and SPM interactions are either focusing or defocusing. For mixed polarizations of two different kinds, $\beta(\xi) \equiv 0$. To simplify the evaluation of this coupled system, we deduce the compact form from the Manakov system as follows [64]

$$\begin{aligned} &iu_\xi + \varphi u_{\tau\tau} - i\gamma u_{\tau\tau\tau} \\ &\quad + i\mu u \mp Du - Cu^+uu + i\alpha_3 u^+u_\tau = 0. \end{aligned} \tag{47}$$

where $u = \binom{u_1}{u_2}$ and $C_1 = C_2 = C$.

The SU(2) rotations are defined by two matrices as

$$\begin{aligned} R_0 &= \begin{pmatrix} \cos\alpha & \sin\alpha \\ -\sin\alpha & \cos\alpha \end{pmatrix}, \\ R_1 &= \begin{pmatrix} e^{iB(\xi)} & -e^{-iB(\xi)} \\ e^{iB(\xi)} & e^{-iB(\xi)} \end{pmatrix}, \end{aligned} \tag{48}$$

where α is a constant and $B(\xi)$ is the real function written down in the form $B(\xi) = -\int \beta(\xi)d\xi$. We defined $\psi = R_1R_0u$ and for the invariant norm, i.e., $u^+u = \psi^+\psi$, we obtain the evolution equation

$$\begin{aligned} &i\psi_\xi + \varphi\psi_{\tau\tau} - i\gamma\psi_{\tau\tau\tau} + i\mu\psi \mp D\psi - C\psi^+\psi\psi \\ &\quad + i\alpha_3\psi^+\psi_\tau - \beta(\xi)\sigma_1\psi = 0, \end{aligned} \tag{49}$$

where $\sigma_j (j = 1,2,3)$ are the standard Pauli matrices. As we construct the rational solution of Eq. (47), we choose it in the form of one component chiral optical rogue wave as

$$u = \Psi(\xi,\tau)\begin{pmatrix}1\\0\end{pmatrix}, \quad \text{where}$$

$$\begin{aligned} \Psi(\xi,\tau) =& \frac{A_0}{\sqrt{-C}}\left[1 - \frac{4 + i8Z(\xi)}{1 + [\sqrt{2}T(\xi,\tau) + 12\nu Z(\xi)]^2 + 4Z(\xi)^2}\right] \\ &\times \exp\{-\mu\xi\}\exp\{iZ(\xi) + i\rho(\xi,\tau)\}, \end{aligned} \tag{50}$$

which is valid for $C < 0$, and where the variables are

$$\begin{aligned} T(\xi,\tau) &= T_1(\xi)\tau + T_0(\xi), \\ \rho(\xi,\tau) &= \rho_1(\xi)\tau + \rho_0(\xi), \\ Z(\xi) &= -\frac{\sqrt{2}\gamma}{4\nu}\int_0^\xi T_1(s)^3 ds \end{aligned} \tag{51}$$

with $\mu = b_3(1 \pm KT_c)$, $T_0(\xi) = cn(\xi,k_2)$, $T_1(\xi) = dn(\xi,k_1)$, $\rho_0(\xi) = sn(\xi,k_4)$, and $\rho_1(\xi) = cn(\xi,k_3)$. The above solution helps us to obtain a parametric family of chiral optical rogue wave solutions of Eq. (49) in the form

$$\psi = \frac{1}{\sqrt{-2C}}\Psi(\xi,\tau)\begin{pmatrix}\cos\alpha e^{iB(\xi)} + \sin\alpha e^{-iB(\xi)} \\ \cos\alpha e^{iB(\xi)} - \sin\alpha e^{-iB(\xi)}\end{pmatrix}. \tag{52}$$

The varying parameters $T_1(\xi)$ and $\rho_1(\xi)$ in this section, excite complex structures which may be useful to control the propagation of chiral optical vector rogue waves.

2. *Second case:* $\Delta = 0$ *and* $CC_{1,2} < 0$

Here, the scattering lengths of the XPM and SPM interactions have the same signs and this allows us to let $\beta(\xi) \equiv 0$.

Therefore, Eqs. (45) are reduced to

$$\begin{aligned} &iw_{1\xi}+\varphi w_{1\tau\tau}-i\gamma w_{1\tau\tau\tau}+i\mu w_1\mp Dw_1\\ &\quad -C(|w_1|^2-|w_2|^2)w_1+i\alpha_3|w_1|^2w_{1\tau}=0,\\ &iw_{2\xi}+\varphi w_{2\tau\tau}-i\gamma w_{2\tau\tau\tau}+i\mu w_2\mp Dw_2\\ &\quad -C(|w_2|^2-|w_1|^2)w_2+i\alpha_3|w_2|^2w_{2\tau}=0, \end{aligned} \tag{53}$$

where $w=\binom{w_1}{w_2}$. The compact form of Eqs. (53) is given by

$$\begin{aligned} &iw_\xi+\varphi w_{\tau\tau}-i\gamma w_{\tau\tau\tau}+i\mu w\mp Dw\\ &\quad -C(w^+\sigma_3 w)\sigma_3 w+i\alpha_3(w^+\sigma_3 w)\sigma_3 w_\tau=0. \end{aligned} \tag{54}$$

For the defined unitary matrices

$$P_0=\begin{pmatrix}\cosh\alpha & \sinh\alpha\\ -\sinh\alpha & \cosh\alpha\end{pmatrix},\qquad P_1=\begin{pmatrix}\sinh\alpha & \cosh\alpha\\ \cosh\alpha & \sinh\alpha\end{pmatrix}, \tag{55}$$

we generate the wave function $\psi=P_jw$ $(j=0,1)$, which solves the system

$$\begin{aligned} &i\psi_{1\xi}+\varphi\psi_{1\tau\tau}-i\gamma\psi_{1\tau\tau\tau}+i\mu\psi_1\mp D\psi_1\\ &\quad -(-1)^jC(|\psi_1|^2-|\psi_2|^2)\psi_1+i\alpha_3|\psi_1|^2\psi_{1\tau}=0,\\ &i\psi_{2\xi}+\varphi\psi_{2\tau\tau}-i\gamma\psi_{2\tau\tau\tau}+i\mu\psi_2\mp D\psi_2\\ &\quad -(-1)^jC(|\psi_1|^2-|\psi_2|^2)\psi_2+i\alpha_3|\psi_2|^2\psi_{2\tau}=0. \end{aligned} \tag{56}$$

The use of a given value for the constant α in the unitary matrixes can reduce the coupled systems (56) to (53) for $|w_1|^2=|w_2|^2$. This imply that the system is purely linear and as consequence, this case can not support chiral optical vector rogue waves of the type $\psi_1\approx\psi_2$.

B. Chiral optical vector rogue waves in the case: $\Delta\neq 0$

We start the study on the case $\Delta\neq 0$ with two polarized electromagnetic waves without linear coupling. We consider $\beta(\xi)\equiv 0$ in the coupled systems (45). As we know the solution of one component chiral optical rogue wave, we can deduce an analog form for two components as follows [43]:

$$\begin{aligned} \psi_1(\xi,\tau)&=a_1\Psi(\xi,\tau),\\ \psi_2(\xi,\tau)&=a_2\Psi(\xi,\tau)\exp(i\delta), \end{aligned} \tag{57}$$

where $\Psi(\xi,\tau)$ is given in relation (50), δ, the constant phase mismatch, a_1 and a_2 are the amplitudes, which yield

$${a_1}^2=\frac{C-C_2}{\Delta},\quad {a_2}^2=\frac{C-C_1}{\Delta}. \tag{58}$$

Here, we let

$$C=\pm 1,\quad C_1=d_1\pm KT_c,\quad C_2=d_2\pm KT_c, \tag{59}$$

where C and $C_{1,2}$ are XPM and SPM nonlinearities and $d_{1,2}$ the arbitrary constants. Relation (58) is the condition for the existence of the synchronized vector rogue waves. The solution (57) obtained in two components describes the propagation of vector rogue waves in chiral optical fibers. We know that a rogue wave is generated by an unstable background and in order to transform our background solution to become unstable, we let $({\psi_1}^{(0)},{\psi_2}^{(0)})=(a_1,a_2)$. By so doing, we choose the solution of Eqs. (45) in the form of a weakly modulated constant background [40,43]

$$\begin{aligned} \psi_j(\xi,\tau)=&[a_j+\alpha_j\exp(iK\xi-i\omega\tau)\\ &+\beta_j\exp(-iK\xi+i\omega\tau)]\\ &\times\exp[-i(C_j{a_j}^2+C{a_{3-j}}^2)\tau], \end{aligned} \tag{60}$$

where a_j is a constant background, α_j and β_j, the amplitudes of the two components, K is the wave number and ω the frequency. Here, we suppose that $\alpha_j,\beta_j\ll a_j(j=1,2)$. The substitution of solution (60) into the coupled systems (45) gives after the linearizing with respect to α_j and β_j, the dispersion relation

$$\begin{aligned} &\gamma^2\omega^6-\gamma(\eta_1+\eta_2)\omega^5+[\eta_1\eta_2-\gamma(\beta_1+\beta_2)]\omega^4\\ &\quad+[\beta_1\eta_2+\beta_2\eta_1-\gamma(\alpha_1+\alpha_2)]\omega^3\\ &\quad+(\beta_1\beta_2+\eta_1\alpha_2+\eta_2\alpha_1)\omega^2+(\beta_1\alpha_2+\beta_2\alpha_1)\omega\\ &\quad+\alpha_1\alpha_2-4{a_1}^2{a_2}^2C^2=0, \end{aligned} \tag{61}$$

where the parameters are

$$\begin{aligned} \phi_{12}&=C_1{a_1}^2+C{a_2}^2,\quad \phi_{22}=C_2{a_2}^2+C{a_1}^2,\\ \eta_1&=\varphi-3\gamma\phi_{12},\quad \eta_2=\varphi-3\gamma\phi_{22},\\ \beta_1&=\phi_{12}+3i\gamma{\phi_{12}}^2-\alpha{a_1}^2,\quad \beta_2=\phi_{22}+3i\gamma{\phi_{22}}^2-\alpha{a_2}^2,\\ \alpha_1&=K+\gamma{\phi_{12}}^3-i\mu\mp D-i\varphi{\phi_{12}}^2+2C_1{a_1}^2\\ &\quad-3\alpha\phi_{12}{a_1}^2+\phi_{12},\\ \alpha_2&=K+\gamma{\phi_{22}}^3-i\mu\mp D-i\varphi{\phi_{22}}^2+2C_2{a_2}^2\\ &\quad-3\alpha\phi_{22}{a_2}^2+\phi_{22}. \end{aligned} \tag{62}$$

Between the roots of the polynomial given in Eq. (61), we should have at least one imaginary root ω to obtain an unstable background and this can be possible under the conditions $C_{1,2}<0$ or $\Delta<0$. Thus, Eq. (61) is the condition of modulational instability of the background. For some specific set of parameters given in Figs. 4–8 captions, we determine the stable and unstable branches of chiral optical rogue waves and indirectly, the existence of vector rogue waves through the dispersion relation given by Eq. (61). We analyze all possible cases for the same and opposite signs of SPM and XPM nonlinearities in the Table I presented in the Appendix.

VI. CHIRAL VECTOR ROGUE WAVES WITH MIXED POLARIZATION IN CHIRAL OPTICAL FIBER

A. Chiral optical rogue waves on mixed polarization without linear coupling

We first consider the case where the XPM and SPM interactions are focusing, i.e., C, $C_{1,2}<0$. Under this consideration, the initial conditions given in the form of exact solution in relation (57), induce the excitation of chiral optical vector rogue waves in the left- and right-hand side [see Figs. 4(a) and 4(b)]. In order to show how sensitive is the evolution of chiral optical rogue wave, we choose another initial conditions with slightly difference on the amplitude. Therefore, we obtain chiral optical vector rogue waves in each hand, where we remark a weak amplitude in the first

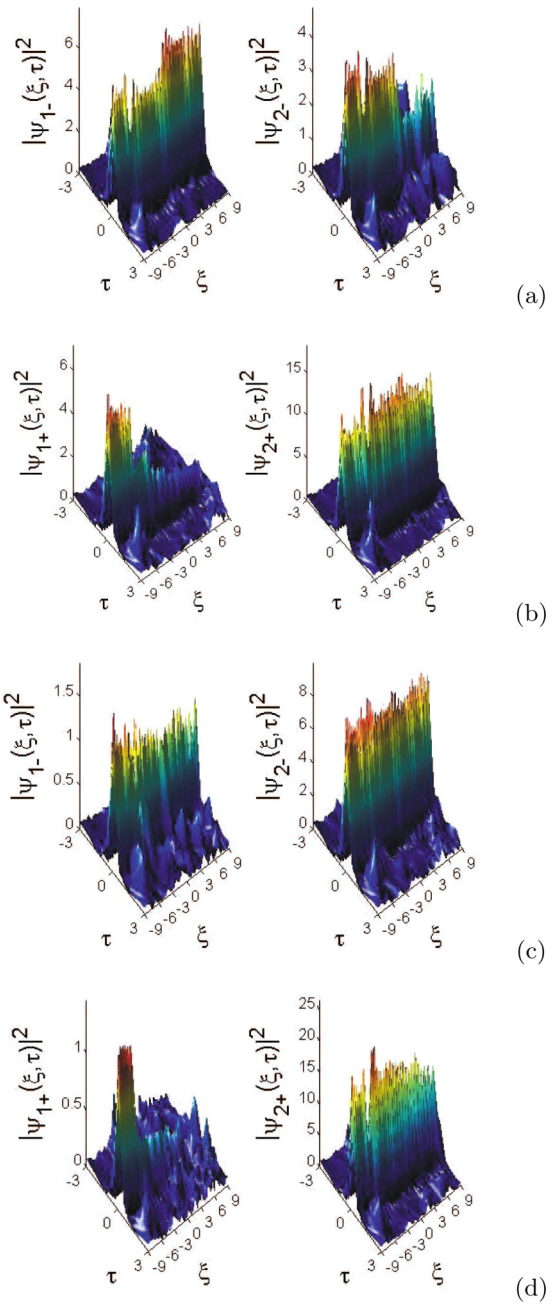

FIG. 4. Chiral optical vector rogue waves of the right- and left-hand intensity $|\psi_{1,2}(\xi,\tau)|^2$ where the parameters are for (a) and (c) $C_1 = -1.6$, $C_2 = -1.8$, $\Delta > 0$, $\mu = b_3(1 - KT_c)$; for (b) and (d) $C_1 = -0.6, C_2 = -0.8, \Delta < 0, \mu = b_3(1 + KT_c)$; with $K = 1, T_c = 0.5, d_1 = -1.1, d_2 = -1.3, \alpha 3 = 0.2, \gamma = 0.02$, $D = 0.6, k_1 = 0.4$, $k_2 = k_4 = 0.6$, $k_3 = 0.5$, $b_3 = 0.01$, and $C = -1$ in each case. At $\xi = -9$, the initial condition takes the form of exact solutions (50) with $\delta = 0$ for (a) and (b) then $\psi_1 = ({a_1}^2 - 0.3)^{1/2}\Psi(\xi,\tau)$, $\psi_2 = ({a_1}^2 + 0.3)^{1/2}\Psi(\xi,\tau)$ for (c) and (d).

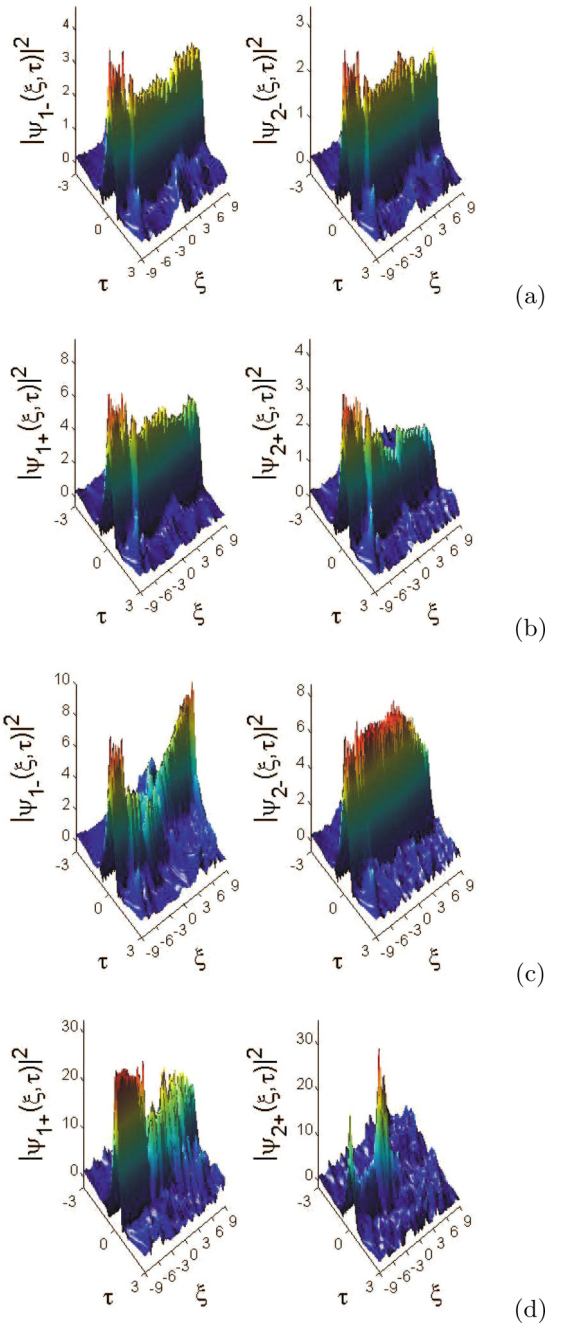

FIG. 5. Chiral optical vector rogue waves of the right- and left-hand intensity $|\psi_{1,2}(\xi,\tau)|^2$ where the parameters are for (a) and (c) $C_1 = -2.5$, $C_2 = -3.0$, $\Delta > 0$, $\mu = b_3(1 - KT_c)$; for (b) and (d) $C_1 = -1.5, C_2 = -2.0, \Delta < 0, \mu = b_3(1 + KT_c)$; with $K = 1, T_c = 0.5, d_1 = -2, d_2 = -2.5, \alpha_3 = 0.2, \gamma = 0.02$, $D = 0.6, k_1 = 0.4$, $k_2 = k_4 = 0.6, k_3 = 0.5$, and $b_3 = 0.01$ in each case; $C = -1$ for (a) and (b); $C = 1$ for (c) and (d). At $\xi = -9$, the initial condition takes the form of exact solutions (50) with $\delta = 0$.

components and a significant one in the second components [see Figs. 4(c) and 4(d)]. In this regard, vector rogue waves most exist in Figs. 4(a) and 4(b) whereas they do not exist in Figs. 4(c) and 4(d). This weak appearance of chiral optical rogue waves in the first components can be understood if we suppose that $|\psi_1|^2 \ll |\psi_2|^2$. In consequence, the function ψ_1 on each hand can be considered as a linear wave function localizes around the minima of the trap potential $U = -|\psi_2|^2$, created by the second component ψ_2, localized around the maxima of the potential barrier. We can conclude that the second components have a self-focusing character that protect them from destructive action of the optical lattice (trapping

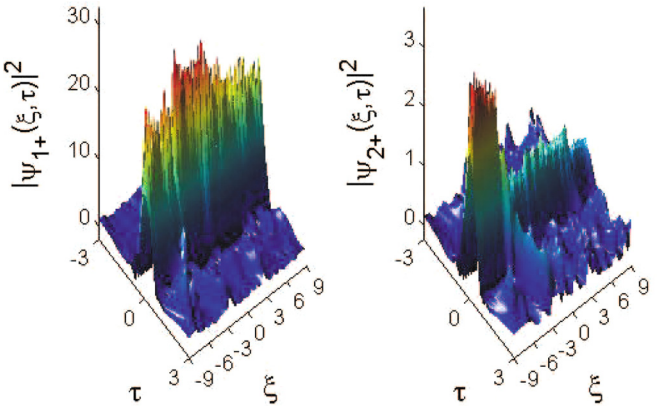

FIG. 6. Nonexistence of chiral optical vector rogue waves of the left-hand and existence of the right-hand intensity $|\psi_{1,2}(\xi,\tau)|^2$ where the parameters are $C_1 = -0.6$, $C_2 = 1.5$, $\Delta < 0$, and $\mu = b_3(1 + KT_c)$ on the right-hand side and $C_1 = -1.6$, $C_2 = 0.5$, $\Delta < 0$ and $\mu = b_3(1 - KT_c)$ on the left-hand side; with $K = 1$, $T_c = 0.5$, $d_1 = -1.1$, $d_2 = 1$, $\alpha_3 = 0.2$, $\gamma = 0.02$, $D = 0.6$, $k_1 = 0.4$, $k_2 = k_4 = 0.6$, $k_3 = 0.5$, $C = -1$, and $b_3 = 0.01$ in each case. At $\xi = -9$, the initial condition takes the form of exact solutions (50) with $\delta = 0$.

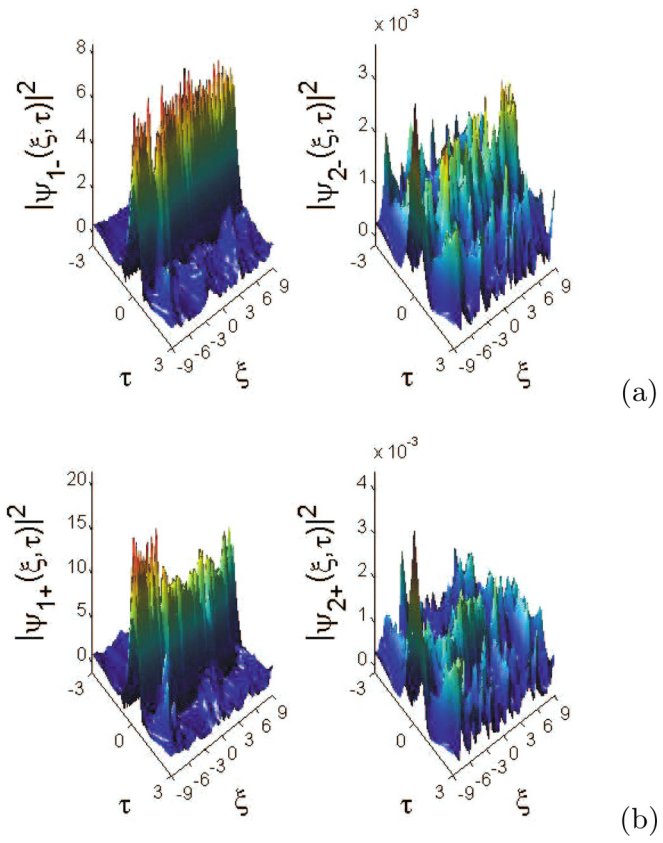

FIG. 7. Chiral optical vector rogue waves of the right- and left-hand intensity $|\psi_{1,2}(\xi,\tau)|^2$ where the parameters are $C_1 = C_2 = 1.96$, and $\mu = b_3(1 - KT_c)$ on the left-hand side and $C_1 = C_2 = -0.96$ and $\mu = b_3(1 + KT_c)$ on the right-hand side; with $K = 1$, $T_c = 0.5$, $d_1 = d_2 = -1.46$ $\alpha_3 = 0.2$, $\gamma = 0.02$, $D = 0.6$, $k_1 = 0.4$, $k_2 = k_4 = 0.6$, $k_3 = 0.5$, $b_3 = 0.01$, and $C = 1$; then $\psi_1 = (-C_1)^{-1/2}\Psi(\xi,\tau)$ and $\psi_2 = 0.02\Psi(\xi,\tau)$ in each case at the origin space $\xi = -9$.

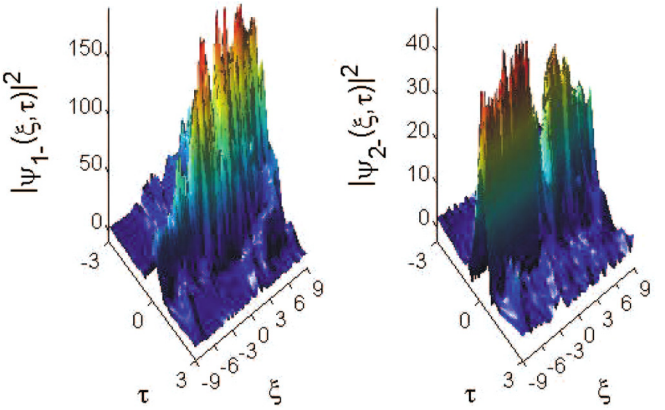

FIG. 8. Existence of chiral vector rogue waves of the left-hand and nonexistence of the right-hand intensity $|\psi_{1,2}(\xi,\tau)|^2$ where the parameters are $C_1 = 0.6$, $C_2 = 0.8$, $\Delta < 0$, and $\mu = b_3(1 - KT_c)$ on the left-hand side and $C_1 = 1.6$, $C_2 = 1.8$, $\Delta > 0$ and $\mu = b_3(1 + KT_c)$ on the right-hand side; with $K = 1$, $T_c = 0.5$, $d_1 = 1.1$, $d_2 = 1.3$, $\alpha_3 = 0.03$, $\gamma = 0.02$, $D = 0.6$, $k_1 = 0.4$, $k_2 = k_4 = 0.6$, $k_3 = 0.5$, $b_3 = 0.01$, and $C = -1$ in each case. At $\xi = -9$, the initial condition takes the form of exact solutions (50) with $\delta = 0$.

potential) whereas the first components, exposed to the self-defocusing character of the potential barriers are trapped in the lattice. Fortunately, there would remain one component in each side in the chiral optical fiber and the transport of information by two components can always take place.

Now, we consider the case depicted in Fig. 5 where we compare the focusing ($C < 0$) and the defocusing ($C > 0$) nature of the XPM nonlinearity with the focusing SPM nonlinearities $C_{1,2} < 0$. We observe in the mixed case of the defocusing nature of the XPM and focusing SPM nonlinearities that the amplitudes are much higher [see Figs. 5(c) and 5(d)] than the ones observed in the unmixed case of defocusing XPM and SPM nonlinearities [see Figs. 5(a) and 5(b)]. An interesting phenomenon occurs on the right-hand side Fig. 5(d) and it can be seen that the components have the same amplitude and the second one is similar to the usual rogue waves, which are localized both in space and time. This special aspect of chiral optical rogue waves, that is, to send two signals through a vector of rogue waves with the same frequency, can help in optic communication domain.

When we choose focusing ($C_1 < 0$) and defocusing ($C_2 > 0$) SPM interactions with focusing XPM interactions, the inverse situation observed in Figs. 4(c) and 4(d) occurs in Figs. 6 where the self-focusing character of the first component, ten times higher than the amplitude of the linear wave function ψ_2, created a trap potential $U = -|\psi_1|^2$ that trap the second component in the lattice. Because of the nonexistence of the left-hand chiral optical rogue waves, this other aspect can help to guide waves in the right-hand side only.

Now, we decide to generate a chiral optical rogue wave in the form of one component with equal SPM interactions, which are either defocusing $C_{1,2} > 0$ or focusing $C_{1,2} < 0$ with defocusing XPM interactions $C > 0$. With slight excitation in the second component as depicted in Fig. 7, we remark that the amplitudes of the second components are too weak in such

a way that we can say, they do no exist and consequently that there is not chiral optical vector rogue waves in both left- and right-hand side. Finally, we can confirm that the defocusing nature of the XPM is responsible for the generation of holes or chiral optical dark rogue waves in the second components and to the unperturbed rogue waves or bright chiral optical rogue waves in the first components. In summary, we can construct a bright-dark vector of rogue waves in chiral optical fiber.

We consider now the case of defocusing interactions of the SPM nonlinearities ($C_{1,2} > 0$) with focusing interactions of XPM nonlinearity ($C < 0$) depicted in Fig. 8, where we can also observe the nonexistence of right-hand chiral optical rogue waves and the propagation of waves in the left-hand side only. Through Fig. 6, we show that vector rogue waves can be guided only in the right-hand side and through Fig. 8 that they can be guided only in the left-hand side. In summary, we can control the propagation direction of vector rogue waves in chiral optical fiber. The presence of several peaks in some profiles in the text is caused by the strong instability of the background and also due to interactions and collisions between components. They are unusual rogue waves also known as Akhmediev breathers or Kuznetsov-Ma soliton, which are not localized in both space and time like usual rogue waves.

B. Chiral optical rogue waves on mixed polarization with linear coupling

We take into account the last term of Eq. (45), $\beta(\xi)$, which is responsible for the exchange between the two wave components. We let N_1 and N_2 as the power in the first and second components, relative to the total power in the system, respectively, in the following form

$$N_1 = \frac{\int |\psi_1(\tau)|^2 d\tau}{\int |\Psi(\tau)|^2 d\tau} = \frac{-1}{2C}\{1 + \sin(2\alpha)\cos[2B(\xi)]\},$$
$$N_2 = \frac{\int |\psi_2(\tau)|^2 d\tau}{\int |\Psi(\tau)|^2 d\tau} = \frac{-1}{2C}\{1 - \sin(2\alpha)\cos[2B(\xi)]\}, \tag{63}$$

where $\psi_{1,2}$ are deduced from Eq. (52), $C = -1$, $\alpha = \frac{\pi}{4} + \frac{n\pi}{2}$ with n being an integer. Now, we choose $B(\xi)$ in the form

$$B(\xi) = \frac{\pi}{4}\left[1 - b\frac{\xi - \xi_0}{\xi_0}\right]. \tag{64}$$

We make a choice where the linear dependance of the phase $B(\xi)$ depends on ξ. Through analytical simulation, we obtain chiral optical vector rogue waves in the left- and right-hand side depicted in Fig. 9. For $b = 1$, the first components in both sides have the behavior of rogons, which after their disappearance, reappear without major shape change in the amplitude [see Figs. 9(a) and 9(b)]. We also remark that all particles are concentrated in the second components in the vicinity of $\xi = 0$. We can see fast oscillations of the background [see Figs. 9(c) and 9(d)] for $b = 15$. We denote in an equal way, the increase of the amplitude in the left-hand and the decrease of the amplitude on the right-hand side and in consequence, this process reveals the presence of FWM, which is responsible for the exchange of energy between components in the system. We show throughout Figs. 4(c) and 4(d) and then through Fig. 6 and Figs. 7(a) and 7(b), how strong XPM interaction can cause the nonexistence of synchronized chiral

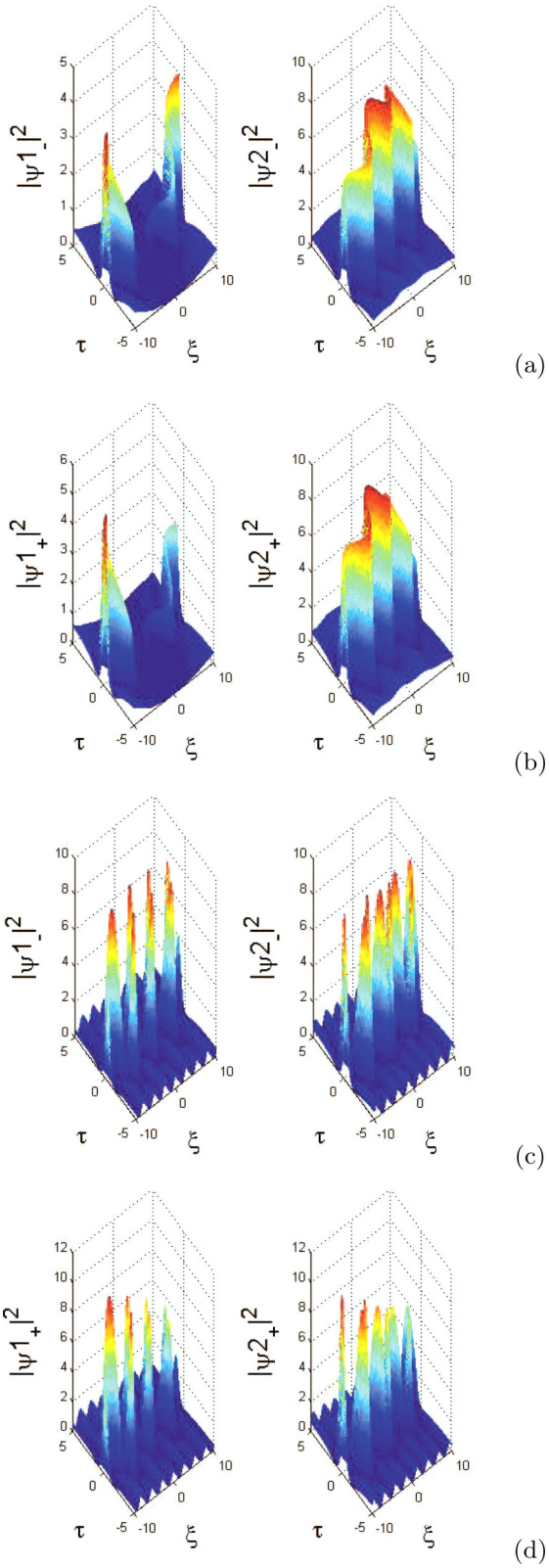

FIG. 9. Chiral vector rogue waves of the right- and left-hand intensity $|\psi_{1,2}(\xi,\tau)|^2$ of Eq. (52) where the parameters are given in Eq. (50), Eq. (51), and Eq. (64) with $\mu = b_3(1 - KT_c)$ on the left-hand side and $\mu = b_3(1 + KT_c)$ on the right-hand side; $b = 1.0$ in (a) and (b) and then $b = 15$ in (c) and (d); with $K = 1$, $T_c = 0.7$, $C = -1$, $\alpha = \pi/4$, $b_3 = 0.01$, $\gamma = 0.03$, $k_1 = 0.4$, $k_2 = 0.6$, $\nu = 0.6$, $\xi_0 = -10$, $T_0(\xi) = cn(\xi,k_2)$, and $T_1(\xi) = dn(\xi,k_1)$ in each case.

vector rogue waves. Nevertheless, we observe that in these cases such waves can exist but with weak amplitude in one component. Then, with the matrices $P_{0,1}$ defined in Eq. (55), we arrive to the equal relation $|\psi_1|^2 = |\psi_2|^2$ from system (56), which describes pure linear dispersive dynamics.

VII. CONCLUSION

In this work, we have derived the NLS-type equation in chiral optical fiber with right- and left-hand nonlinear polarization. The model is used to describe the propagation of optical rogue waves in chiral fiber. We have used the symmetry reduction and the modified Darboux transformation to generate the rational solutions. In so doing, we have constructed the first- and second-order chiral optical rogue waves from the chiral NLS equation with variable and constant coefficients, respectively. In order to show the influence of optical activity on the propagation of rogue waves, we have chosen Jacobian elliptic functions for good stability of the waves. We have recorded from analytical results that in chiral optical fiber we obtained two components, left- and right-hand intensities. We have observed that the shape and the amplitude of chiral optical rogue waves change with the increase of the chiral parameter. This allows us to conclude that the slight change of the amplitude is due to the optical activity and TWM effects. We have performed our study by using chiral CNLS equations and with the help of MATLAB, we have generated the chiral optical vector rogue waves with four components showing, through the exchange of energy, the FWM effect. In the case of focusing and defocusing XPM interactions, we have found unusual rogue waves such as Akhmediev breathers or the Kuznetsov-Ma soliton. Then, we have shown the influence of optical activity on different profiles. We have noticed that the destruction of one component contributes to the perturbations that lead to modulation instability and that the defocusing nature of XPM generates chiral optical dark rogue waves. We have also shown that positive and negative scattering lengths can generate a potential barrier for one component in the left- or right-hand side. Finally, we can control and guide the propagation direction of chiral optical vector rogue waves either in the left-hand or in the right-hand side for some specific set of parameters, including chiral parameter. This aspect can find applications in telecommunication and in many other physical systems.

APPENDIX

In this Appendix, we present the derivation of Eq. (3).

Equation (3) is reduced in x, y, and z directions, respectively, as follows

$$
\begin{aligned}
&-2jK_z\frac{\partial E_x}{\partial z} - {K_z}^2E_x + \mu_0\varepsilon_0{T_c}^2\left(\omega^2{K_z}^2E_x + 2jK_z\omega^2\frac{\partial E_x}{\partial z} - 2j{K_z}^2\omega\frac{\partial E_x}{\partial t}\right)\\
&= (\mu_0\varepsilon_0 + \mu_0\varepsilon_2|\vec{E}|)\left(2j\omega\frac{\partial E_x}{\partial t} - \omega^2E_x\right) + \mu_0\sigma\left(\frac{\partial E_x}{\partial t} + j\omega E_x\right) + (2\mu_0\varepsilon_0T_c + \mu_0\varepsilon_2T_c|\vec{E}|^2)\\
&\quad\times\left(\omega^2\frac{\partial E_y}{\partial z} + jK_z\left(2j\omega\frac{\partial E_x}{\partial t} - \omega^2E_y\right)\right) + \mu_0\sigma T_c\left[-j\omega\frac{\partial E_y}{\partial z} + jK_z\left(\frac{\partial E_y}{\partial t} + j\omega E_y\right)\right] \qquad \text{(A1)}\\
&-2jK_z\frac{\partial E_y}{\partial z} - {K_z}^2E_y + \mu_0\varepsilon_0{T_c}^2\left(\omega^2{K_z}^2E_y + 2jK_z\omega^2\frac{\partial E_y}{\partial z} - 2j{K_z}^2\omega\frac{\partial E_y}{\partial t}\right)\\
&= (\mu_0\varepsilon_0 + \mu_0\varepsilon_2|\vec{E}|)\left(2j\omega\frac{\partial E_y}{\partial t} - \omega^2E_y\right) + \mu_0\sigma\left(\frac{\partial E_y}{\partial t} + j\omega E_y\right) + (2\mu_0\varepsilon_0T_c + \mu_0\varepsilon_2T_c|\vec{E}|^2)\\
&\quad\times\left[-\omega^2\frac{\partial E_x}{\partial z} - jK_z\left(2j\omega\frac{\partial E_x}{\partial t} - \omega^2E_x\right)\right] + \mu_0\sigma T_c\left[j\omega\frac{\partial E_x}{\partial z} - jK_z\left(\frac{\partial E_x}{\partial t} + j\omega E_x\right)\right] \qquad \text{(A2)}\\
&[-\omega^2(2\mu_0\varepsilon_0T_c + \mu_0\varepsilon_2T_c|\vec{E}|^2) + j\omega\mu_0\sigma T_c]\left(\frac{\partial E_y}{\partial x} - \frac{\partial E_x}{\partial y}\right) = 0. \qquad \text{(A3)}
\end{aligned}
$$

Equation (A3) leads to

$$\frac{\partial E_y}{\partial x} = \frac{\partial E_x}{\partial y} = cst, \quad E_y = E_y(z,t), \quad E_x = E_x(z,t). \qquad \text{(A4)}$$

Having multiplied Eq. (A2) by $\pm j$, we do the addition of Eqs. (A1) and (A2) where we also consider the paraxial approximation

$$\left|\frac{\partial E_x}{\partial t}\right| \ll |2j\omega E_x|, \quad \left|\frac{\partial^2 E_y}{\partial z^2}\right| \ll |2j\omega E_y|. \qquad \text{(A5)}$$

Therefore, the novel form of wave equation can be written as

$$
\begin{aligned}
&\left[\pm j[(2\mu_0\varepsilon_0T_c + \mu_0\varepsilon_2T_c|\vec{E}|^2)\omega^2 - j\omega\mu_0\sigma T_c] - 2jK_z + 2jK_z\omega^2\mu_0\varepsilon_0{T_c}^2\right]\frac{\partial\psi_{R,L}}{\partial z} + \left[-{K_z}^2 + \mu_0\varepsilon_0{T_c}^2\omega^2{K_z}^2\right.\\
&\left.+\omega^2(\mu_0\varepsilon_0 + \mu_0\varepsilon_2|\vec{E}|^2) - j\omega\mu_0\sigma \pm j(-jK_z\omega^2(2\mu_0\varepsilon_0T_c + \mu_0\varepsilon_2T_c|\vec{E}|^2) - K_z\omega\mu_0\sigma T_c)\right]\psi_{R,L}\\
&+\left[-2j\times K_z^2\omega\mu_0\varepsilon_0{T_c}^2 - 2j\omega(\mu_0\varepsilon_0 + \mu_0\varepsilon_2|\vec{E}|^2)\right]\frac{\partial\psi_{R,L}}{\partial t} = 0, \qquad \text{(A6)}
\end{aligned}
$$

TABLE I. Occurrence of modulation instability and chiral vector rogue waves for mixed cases of SPM and XPM interactions.

SPM interactions	XPM interactions	Unstable Branches	Stable Branches	Chiral vector rogue waves
$C_{1,2} < 0$	$-: C > C_{1,2}, \Delta > 0$ $+: C < C_{1,2}, \Delta < 0$	$-: 4$ $+: 4$	$-: 2$ $+: 2$	$-: exist$ $+: not\ exist$
	$-: \lvert C\rvert < \lvert C_{1,2}\rvert, \Delta > 0$ $+: \lvert C\rvert < \lvert C_{1,2}\rvert, \Delta > 0$	$-: 4$ $+: 4$	$-: 2$ $+: 2$	$-: exist$ $+: exist$
	$-: C < \lvert C_{1,2}\rvert, \Delta > 0$ $+: C > \lvert C_{1,2}\rvert, \Delta < 0$	$-: 4$ $+: 4$	$-: 2$ $+: 2$	$-: not\ exist$ $+: not\ exist$
$C_{1,2} > 0$	$-: C > C_{1,2}, \Delta < 0$ $+: C < C_{1,2}, \Delta > 0$	$-: 4$ $+: 3$	$-: 2$ $+: 3$	$-: not\ exist$ $+: not\ exist$
	$-: \lvert C\rvert > C_{1,2}, \Delta < 0$ $+: \lvert C\rvert < C_{1,2}, \Delta > 0$	$-: 4$ $+: 4$	$-: 2$ $+: 2$	$-: exist$ $+: not\ exist$
	$-: C < -C_{1,2}, \Delta < 0$ $+: C > -C_{1,2}, \Delta > 0$	$-: 3$ $+: 3$	$-: 3$ $+: 3$	$-: exist$ $+: not\ exist$
$C_1 < 0, C_2 > 0$	$-: C < C_{1,2}, \Delta < 0$ $+: C < C_{1,2}, \Delta < 0$	$-: 5$ $+: 4$	$-: 1$ $+: 2$	$-: not\ exist$ $+: exist$

where $\psi_{R,L} = E_x \pm jE_y$. Then the reference changes is out to be

$$\begin{cases} \psi_R = E_x + jE_y \\ \psi_L = E_x - jE_y \end{cases} \quad \begin{cases} E_x = \frac{\psi_R + \psi_L}{2} \\ E_y = \frac{\psi_R - \psi_L}{2}. \end{cases} \tag{A7}$$

The division of Eq. (A6) by $-2K_z$ yields

$$\begin{aligned} & j\left(1 - {K_0}^2 {T_c}^2\right)\frac{\partial \psi_{R,L}}{\partial z} \mp j\frac{{K_0}^2 T_c}{K_z}\frac{\partial \psi_{R,L}}{\partial z} + j\frac{\omega\mu_0\varepsilon_2}{K_z}|\psi_{R,L}|^2\frac{\partial \psi_{R,L}}{\partial t} \mp j\frac{\mu_0\varepsilon_2\omega^2 T_c}{2K_z}|\psi_{R,L}|^2\frac{\partial \psi_{R,L}}{\partial z} \\ & + j\frac{K_0}{K_z c}\left(1 + {K_z}^2 {T_c}^2\right)\frac{\partial \psi_{R,L}}{\partial t} \mp \frac{j\omega\mu_0\sigma T_c}{2}\psi_{R,L} + \frac{1}{2}\left(K_z - K_z {K_0}^2 {T_c}^2 - \frac{{K_0}^2}{K_z}\right)\psi_{R,L} - \frac{\mu_0\varepsilon_2\omega^2}{2K_z} \\ & \times |\psi_{R,L}|^2\psi_{R,L} \mp \frac{\omega^2}{2}(\mu_0\varepsilon_2 T_c|\psi_{R,L}|^2)\psi_{R,L} + j\frac{\omega\mu_0\sigma}{2K_z}\psi_{R,L} \mp {K_0}^2 T_c\psi_{R,L} \mp \frac{\omega\mu_0\sigma T_c}{2K_z}\frac{\partial \psi_{R,L}}{\partial z} = 0, \end{aligned} \tag{A8}$$

where

$$K_0 = \frac{\omega}{c}, \quad \mu_0\varepsilon_0 c^2 = 1. \tag{A9}$$

The dispersion relation is given by

$$K_z = \frac{K_0}{1 \pm K_0 T_c}. \tag{A10}$$

For ${K_0}^2 {T_c}^2 \ll 1$, we get $K_z = K_0$. By neglecting the nonlinear diffraction, the second and the last terms of Eq. (A8), and for the following set of parameters

$$\begin{aligned} & v^2 = \frac{1}{\mu_0\varepsilon_0}, \quad \alpha = \mu_0\sigma, \quad \beta = \mu_0\varepsilon_2 \\ & K_0 = \frac{\omega}{v}, \quad z^* = \frac{z}{1 - {K_0}^2 {T_c}^2}, \end{aligned} \tag{A11}$$

Eq. (A8) takes the form

$$\begin{aligned} & j\frac{\partial \psi_{R,L}}{\partial z^*} + j\frac{1}{v}\frac{\partial \psi_{R,L}}{\partial t} + j\frac{\omega\alpha}{2K_0}\psi_{R,L} \mp {K_0}^2 T_c\psi_{R,L} \\ & - \frac{\beta\omega^2}{2K_0}|\psi_{R,L}|^2\psi_{R,L} \mp \frac{j\omega\alpha T_c}{2}\psi_{R,L} \mp \frac{\omega^2\beta T_c}{2} \\ & \times |\psi_{R,L}|^2\psi_{R,L} + \frac{j\omega\beta}{K_0}|\psi_{R,L}|^2\frac{\partial \psi_{R,L}}{\partial t} = 0. \end{aligned} \tag{A12}$$

If we let

$$\psi_{R,L} = \phi, \quad K = K_0 = K_z, \tag{A13}$$

Eq. (A11) yields

$$j\frac{\partial\phi}{\partial z^*}+j\frac{1}{v}\frac{\partial\phi}{\partial t}+j\frac{\omega\alpha}{2K_0}(1\mp KT_c)\phi - \frac{\beta\omega^2}{2K_0}(1\mp KT_c)|\phi|^2\phi\mp K^2T_c\phi+j\frac{\omega\beta}{K_0}|\phi|^2\frac{\partial\phi}{\partial t}=0. \tag{A14}$$

The Taylor series of the wave number $K(\omega)$ at the third order and the Fourier transform of $\Delta\omega$ and ΔK help to express in an approximate form, the second term of Eq. (A13) as

$$j\frac{1}{v}\frac{\partial\phi}{\partial t}=j\frac{1}{v_g}\frac{\partial\phi}{\partial t}+\frac{1}{2}K''\frac{\partial^2\phi}{\partial t^2}-j\frac{1}{6}K'''\frac{\partial^3\phi}{\partial t^3}, \tag{A15}$$

where

$$K''=\frac{\partial^2K}{\partial\omega^2},\quad K'''=\frac{\partial^3K}{\partial\omega^3},\quad K'=\frac{1}{v_g}=\frac{\partial K}{\partial\omega}. \tag{A16}$$

Then, for the following change of variable

$$\begin{cases}t'=t-\frac{1}{v_g}z^*\\ z'=z^*\end{cases}\Rightarrow\begin{cases}\frac{\partial}{\partial t}\rightarrow\frac{\partial}{\partial t'}\\ \frac{\partial}{\partial z^*}\rightarrow\frac{\partial}{\partial z'}-\frac{1}{v_g}\frac{\partial}{\partial t'}\end{cases}, \tag{A17}$$

Eq. (A14) stands for

$$j\frac{\partial\phi}{\partial z'}+\frac{1}{2}K'\frac{\partial^2\phi}{\partial t'^2}-j\frac{1}{6}K'''\frac{\partial^3\phi}{\partial t'^3}+j\frac{\omega\alpha}{2K_0}(1\mp KT_c)\phi - \frac{\beta\omega^2}{2K_0}(1\mp KT_c)|\phi|^2\phi\mp K^2T_c\phi+j\frac{\omega\beta}{K_0}|\phi|^2\frac{\partial\phi}{\partial t'}=0. \tag{A18}$$

In the table below, we analyze the specific cases of SPM and XPM interactions when they have the same and opposite signs.

[1] A. Hasegawa and F. Tappert, Appl. Phys. Lett. **23**, 142 (1973).
[2] L. F. Mollenauer, R. H. Stolen, and J. P. Gordon, Phys. Rev. Lett. **45**, 1095 (1980).
[3] R. H. Stolen, L. F. Mollenauer, and W. J. Tomlison, Opt. Lett. **8**, 186 (1983).
[4] L. F. Mollenauer, R. H. Stolen, J. P. Gordon, and W. J. Tomlinson, Opt. Lett. **8**, 289 (1983).
[5] N. N. Akmediev and E. A. Ostrovskaya, Opt. Commun. **132**, 190 (1996).
[6] M. V. Tratnik and J. E. Sipe, Phys. Rev. A **38**, 2011 (1988).
[7] N. N. Akhmediev, V. M. Eleonskii, N. E. Kulagin, and L. P. Shil'nikov, Pis'ma Zh. Sov. Tech. Phys. Lett. **15**, 587 (1989).
[8] M. Haelterman and A. Sheppard, Phys. Rev. E **49**, 3376 (1994).
[9] B. Bai, Y. Svirko, J. Turunen, and T. Vallius, Phys. Rev. A **76**, 023811 (2007).
[10] H. Torres-Silva and M. Zamorano, Math. Comput. Sim. **62**, 149 (2003).
[11] L. Poladian, M. Straton, A. Doccherty, and A. Argyros, Opt. Express **19**, 968 (2011).
[12] B. Bai, J. Laukkanen, A. Lehmuskero, and J. Turunen, Phys. Rev. B **81**, 115424 (2010).
[13] H. Torres-Silva, C. Villarroel, P. H. Sakanaka, and N. Reggiani, Pramana–J. Phys. **49**, 431 (1997).
[14] Y. Chen and J. Atai, J. Opt. Soc. Am. B **14**, 2365 (1997).
[15] H. Torres-Silva and M. Zamorano Lucero, Pramana–J. Phys. **62**, 37 (2004).
[16] P. D. Maker, R. W. Terhune, and C. M. Savage, Phys. Rev. Lett. **12**, 507 (1964).
[17] P. K. Choudhury and T. Yoshino, Optik **113**, 89 (2002).
[18] A. Argyros, J. Pla, F. Ladouceur, and L. Poladian, Opt. Express **17**, 15983 (2009).
[19] Kh. S. Singh, P. Khastgir, S. P. Ojha, and P. K. Choudhury, J. Phys. Soc. Jpn. **62**, 1978 (1993).
[20] N. S. Pujari, M. R. Kulkarni, M. C. J. Large, I. M. Bassett, and S. Ponrathnam, J. Appl. Polym. Sci. **98**, 58 (2005).
[21] A. Argyros, M. Straton, A. Docherty, E. H. Min, Z. Ge, K. H. Wong, F. Ladouceur, and L. Poladin, Frontiers Optoelectron. China **3**, 67 (2010).
[22] C. Dai, Y. Wang, and X. Zang, Opt. Express **22**, 29862 (2014).
[23] D. H. Peregrine, J. Aust. Math. Soc. Series B, Appl. Math. **25**, 16 (1983).
[24] N. Akhmediev and V. I. Korneev, Theor. Math. Phys. **69**, 1089 (1986).
[25] E. A. Kuznetsov, Dokl. Akad. Nauk SSSR **236**, 575 (1977).
[26] Z. Y. Yan, Phys. Lett. A **374**, 672 (2010).
[27] N. Akhmediev, A. Ankiewicz, and M. Taki, Phys. Lett. A **373**, 675 (2009).
[28] N. Akhmediev, J. M. Soto-Crespo, and A. Ankiewicz, Phys. Lett. A **373**, 2137 (2009).
[29] D. D. Estelle Temgoua and T. C. Kofane, Phys. Rev. E **91**, 063201 (2015).
[30] J. M. Dudley, G. Genty, F. Dias, B. Kibler, and N. Akhmediev, Opt. Express **17**, 21497 (2009).
[31] A. N. Ganshin, V. B. Efimov, G. V. Kolmakov, L. P. Mezhov-Deglin, and P. V. E. McClintock, Phys. Rev. Lett. **101**, 065303 (2008).
[32] A. N. W. Hone, J. Phys. A: Math. Gen. **30**, 7473 (1997).
[33] A. Montina, U. Bortolozzo, S. Residori, and F. T. Arecchi, Phys. Rev. Lett. **103**, 173901 (2009).
[34] P. Müller, C. Garrett, and A. Osborne, Oceanography **18**, 66 (2005).
[35] A. Nakamura and R. Hirota, J. Phys. Soc. Jpn. **54**, 491 (1985).
[36] M. Noumi and Y. Yamada, Nagoya Math. J. **153**, 53 (1999).
[37] D. R. Solli, C. Ropers, P. Koonath, and B. Jalali, Nature (London) **450**, 1054 (2007).
[38] M. Ballav and A. R. Chowdhury, Chaos **17**, 013102 (2007).
[39] T. B. Benjamin and J. E. Fier, J. Fluid Mech. **27**, 417 (1967).
[40] N. A. Kostov, V. Z. Enolskii, V. S. Gerdjikov, V. V. Konotop, and M. Salerno, Phys. Rev. E **70**, 056617 (2004).
[41] Y. V. Bludov, V. V. Konotop, and N. Akhmediev, Opt. Lett. **34**, 3015 (2009).
[42] M. Shats, H. Punzmann, and H. Xia, Phys. Rev. Lett. **104**, 104503 (2010).
[43] Y. V. Bludov, V. V. Konotop, and N. Akhmediev, Eur. Phys. J. ST **185**, 169 (2010).
[44] Y. V. Bludov, V. V. Konotop, and N. Akhmediev, Phys. Rev. A **80**, 033610 (2009).

[45] S. Loomba, H. Kaur, R. Gupta, C. N. Kumar, and T. S. Raju, Phys. Rev. E **89**, 052915 (2014).
[46] E. Wamba, K. Porsezian, A. Mohamadou, and T. C. Kofane, Phys. Lett. A **377**, 262 (2013).
[47] Y. V. Bludov, R. Driben, V. V. Konotop, and B. A. Malomed, J. Opt. **15**, 064010 (2013).
[48] L. Wen, L. Li, Z. D. Li, S. W. Song, X. F. Zhang, and W. M. Liu, Eur. Phys. J. D **64**, 473 (2011).
[49] J. Atangana, B. G. O. Essama, F. Biya-Motto, B. Mokhtari, N. C. Eddeqaqi, and T. C. Kofane, J. Mod. Opt. **62**, 392 (2015).
[50] B. G. O. Essama, J. Atangana, F. Biya-Motto, B. Mokhtari, N. C. Eddeqaqi, and T. C. Kofane, Opt. Commun. **331**, 334 (2014).
[51] A. Laktakia and V. K. Varadan, *Time-Harmonic Electromagnetic Fields in Chiral Media*, Lecture Notes in Physics, Vol. 335 (Springer, Berlin, 1985).
[52] Z. Yan and C. Dai, J. Opt. **15**, 064012 (2013).
[53] G. W. Bluman and S. Kumei, *Symmetries and Differential Equations* (Springer, New York, 1989).
[54] G. W. Bluman and Z. Y. Yan, Eur. J. Appl. Math. **16**, 239 (2005).
[55] B. Guo, L. Ling, and Q. P. Liu, Phys. Rev. E **85**, 026607 (2012).
[56] Zhenya Yan, V. V. Konotop, and N. Akhmediev, Phys. Rev. E **82**, 036610 (2010).
[57] W.-P. Zhong, M. R. Belic, and T. Huang, Phys. Rev. E **87**, 065201 (2013).
[58] A. Ankiewicz, J. M. Soto-Crespo, and N. Akhmediev, Phys. Rev. E **81**, 046602 (2010).
[59] N. Akhmediev, A. Ankiewicz, and J. M. Soto-Crespo, Phys. Rev. E **80**, 026601 (2009).
[60] E. N. Tsoy, A. Ankiewicz, and N. Akhmediev, Phys. Rev. E **73**, 036621 (2006).
[61] A. T. Avelar, D. Bazeia, and W. B. Cardoso, Phys. Rev. E **79**, 025602 (2009).
[62] N. Akhmediev, V. M. Eleonskii, and N. E. Kulagin, Sov. Phys. JETP **89**, 1542 (1985).
[63] P. F. Byrd and M. D. Friedman, *Handbook of Elliptic Integrals for Engineers and Scientists*, 2nd ed. (Springer, Berlin, 1971).
[64] S. V. Manakov, Zh. Eksp. Teor. Fiz. **67**, 543 (1974).